TECHNICAL REPORT AMR-SS-06-09

IMPACT SHOCK SENSITIVITY OF A TATB BASED EXPLOSIVE RELEVANT TO SPECIFIC HEAT PROPERTIES

James P. Billingsley

System Simulation and Development Directorate
Aviation and Missile Research, Development, and Engineering Center

February 2006

Approved for public release; distribution is unlimited.

DESTRUCTION NOTICE

FOR CLASSIFIED DOCUMENTS, FOLLOW THE PROCEDURES IN DoD 5200.22-M, INDUSTRIAL SECURITY MANUAL, SECTION II-19 OR DoD 5200.1-R, INFORMATION SECURITY PROGRAM REGULATION, CHAPTER IX. FOR UNCLASSIFIED, LIMITED DOCUMENTS, DESTROY BY ANY METHOD THAT WILL PREVENT DISCLOSURE OF CONTENTS OR RECONSTRUCTION OF THE DOCUMENT.

DISCLAIMER

THE FINDINGS IN THIS REPORT ARE NOT TO BE CONSTRUED AS AN OFFICIAL DEPARTMENT OF THE ARMY POSITION UNLESS SO DESIGNATED BY OTHER AUTHORIZED DOCUMENTS.

TRADE NAMES

USE OF TRADE NAMES OR MANUFACTURERS IN THIS REPORT DOES NOT CONSTITUTE AN OFFICIAL ENDORSEMENT OR APPROVAL OF THE USE OF SUCH COMMERCIAL HARDWARE OR SOFTWARE.

REPORT DOCUMENTATION PAGE				Form Approved OMB No. 074-0188
Public reporting burden for this collection of information is estimated to average 1 hour per response, including the time for reviewing instructions, searching existing data sources, gathering and maintaining the data needed, and completing and reviewing this collection of information. Send comments regarding this burden estimate or any other aspect of this collection of information, including suggestions for reducing this burden to Washington Headquarters Services, Directorate for Information Operations and Reports, 1215 Jefferson Davis Highway, Suite 1204, Arlington, VA 22202-4302, and to the Office of Management and Budget, Paperwork Reduction Project (0704-0188), Washington, DC 20503				
1. AGENCY USE ONLY	2. REPORT DATE February 2006	3. REPORT TYPE AND DATES COVERED Final		
4. TITLE AND SUBTITLE Impact Shock Sensitivity of a TATB Based Explosive Relevant to Specific Heat Properties				5. FUNDING NUMBERS
6. AUTHOR(S) James P. Billingsley				
7. PERFORMING ORGANIZATION NAME(S) AND ADDRESS(ES) Commander, U.S. Army Research, Development, and Engineering Command ATTN: AMSRD-AMR-SS-EG Redstone Arsenal, AL 35898				8. PERFORMING ORGANIZATION REPORT NUMBER TR-AMR-SS-06-09
9. SPONSORING / MONITORING AGENCY NAME(S) AND ADDRESS(ES)				10. SPONSORING / MONITORING AGENCY REPORT NUMBER
11. SUPPLEMENTARY NOTES				
12a. DISTRIBUTION / AVAILABILITY STATEMENT Approved for public release; distribution is unlimited.				12b. DISTRIBUTION CODE A

13. ABSTRACT *(Maximum 200 Words)*

This report is a supplementary follow-on to U.S. Army Missile Command (MICOM) TR-RD-SS-95-2, and Aviation and Missile Command (AMCOM) TR-RD-SS-99-8 that related plane impact shock sensitivity of CHNO energetic material to specific heat (Cp) per average atom magnitude and reactive temperature (T_R) conditions. Specifically, plane shock energy input equal to the thermal vibratory energy increment (this is the area under the Cp versus T data curve between experimental temperature, T_{EXP}, conditions and reactive temperature conditions) is sufficient to cause shock induced reactions, up to and including detonation in energetic materials. This is demonstrated at four different test temperatures (T_{EXP}) for PBX-9502.

14. SUBJECT TERMS			15. NUMBER OF PAGES
Detonation thresholds, shock reaction criteria, shock loaded explosives, specific heat, reactive temperatures, TATB, PBX-9502			57
			16. PRICE CODE
17. SECURITY CLASSIFICATION OF REPORT	18. SECURITY CLASSIFICATION OF THIS PAGE	19. SECURITY CLASSIFICATION OF ABSTRACT	20. LIMITATION OF ABSTRACT
UNCLASSIFIED	UNCLASSIFIED	UNCLASSIFIED	SAR

NSN 7540-01-280-5500

Standard Form 298 (Rev. 2-89)
Prescribed by ANSI Std. Z39-18
298-102

ACKNOWLEDGEMENTS

The author gratefully acknowledges the assistance of Davidson Technologies, Inc. personnel in preparing this report. Ms. Judy Smith typed the manuscript and Mr. Chris Pitts and Mr. Brent Deerman assisted in preparing the computer-drawn graphs.

TABLE OF CONTENTS

		Page
I.	INTRODUCTION	1
II.	ANALYSIS	2
III.	APPLICATIONS	5
	A. PBX-9502 Experimental Thermal Data	5
	B. PBX-9502 Experimental 1-D Impact Shock Data	7
	C. PBX-9502 $\Delta(v.e.)_{TR}$, $U_{P_{CR}}$, and $P_{S_{CR}}$ Results	9
IV.	DISCUSSION	10
V.	CONCLUSIONS	12
VI.	RECOMMENDATIONS	13
	REFERENCES	31
	APPENDIX A: COMPUTATION OF M_{AV} AND D_{1AV} FOR PBX-9502	A-1
	APPENDIX B: SPECIFIC HEAT (C_P) CONVERSION RELATIONS	B-1

LIST OF TABLES

Table	Title	Page
1.	Thermal Properties of TBX-9502	14
2.	PBX – 9502 Specific Heat (C_P)	15
3.	Impact Shock Loaded Material Data for $U_S = C_O + S\ U_P$ Relation	16
4.	PBX-9502 U_P Versus X_D Information from Popolato Plots in References [6] and]8] for T_{EXP} = -55 °C = 218 °K	17
5.	PBX-9502 Estimated Impact Shock Induced Threshold Information From U_P, V_S, X_D Data	18
6.	Computation of $U_{p_{CR1}}$ and $U_{p_{CR2}}$	19
7.	Computation of $U_{s_{CR}}$ and $P_{s_{CR}}$	20

LIST OF ILLUSTRATIONS

Figure	Title	Page
1.	Specific Heat per Average Atom for PBX-9502, TATB, and RDX	21
2.	U_P Versus X_D for PBX-9502 at T_{EXP} = - 55 ºC = 218 ºK	22
3.	U_p Versus X_D for PBX-9502 at T_{EXP} = Ambient Room Temperature (R T)	23
4.	U_p Versus X_D for PBX-9502 at T_{EXP} = 75 ºC = 348 ºK	24
5.	U_p Versus X_D for PBX-9502 at T_{EXP} = 252 ºC = 525 ºK	25
6.	U_p Versus t_D for PBX-9502 at T_{EXP} = RT Conditions	26
7.	U_p Versus t_D for PBX-9502 at T_{EXP} = 75 ºC = 348 ºK	27
8.	U_p Versus t_D for PBX-9502 at T_{EXP} = 252 ºC = 525 ºK	28
9.	Detonation Threshold ($U_{P_{DT}}$) and Theoretical ($U_{P_{CR}}$, No ΔH_F) Results for PBX-9502, T_R = 396 ˚C = 669 ˚K = T_{EXPL}	29

I. INTRODUCTION

Essentially, the area Δ (v.e.)$_{TR}$ under the Specific Heat (C_P) versus Temperature (T) plots between temperature limits, Experimental Test Temperature (T_{EXP}) and Reactive Temperature (T_R) is a measure of how much atomic vibratory energy explosives can absorb before a reaction occurs. The reaction may be melting, phase change, decomposition, burning, or even detonation. Thus, to a good approximation, it could be expected that if Δ(v.e.)$_{TR}$ amount of energy is suddenly added via impact shock loading, then a reaction may occur.

This Δ (v.e.)$_{TR}$ concept, that impact shock sensitivity or shock induced reactivity of energetic materials could be related to their specific heat (C_P) variation with temperature, was demonstrated in References [1] and [2] for RDX, TETRYL, PETN, TNT, and TATB, which are basic secondary reactive compounds.

In References [3] and [4], the Δ (v.e.)$_{TR}$ ideas were demonstrated for HMX and HNS which are also important basic secondary explosive compounds. The impact shock response of these seven compounds ranges from very insensitive to highly sensitive. Most of these seven basic energetic compounds have been the main ingredient of useful explosive mixtures.

One such mixture is the plastic bonded explosive designated as PBX-9502 that is 95 percent TATB and 5 percent KEL-F800 [5, 6]. PBX-9502 has been rather extensively tested via one-dimensional shock loading at various temperatures [7, 8, 9], and its thermal characteristics have also been experimentally explored [10, 11, 12]. Much of this important information has been collected, reported, or at least mentioned, in Reference [6]. Some of these data for PBX-9502 are listed in Tables 1, 2, 3, and 4.

Utilizing this information, Δ (v.e.)$_{TR}$ concept computations were made for PBX-9502. The exploratory comparative results for this important energetic material provides considerable affirmation and support for the Δ (v.e.)$_{TR}$ theory of impact shock sensitivity.

General details of the exploratory computations and experimental data comparisons involved in a general Δ (v.e.)$_{TR}$ assessment are contained in the following sections.

II. ANALYSIS

This section contains excerpts from similar sections in References [1] and [3], which should be consulted for additional details.

For some explosives, a good estimate of the critical particle velocity, U_{PCR} , where a reaction (or detonation) occurs is:

$$U_{PCR1} = \sqrt{\frac{\Delta(v.e.)_{TR}}{m_{AV}}} \qquad (1)$$

In some circumstances, a better estimate of the critical particle velocity is:

$$U_{PCR2} = \sqrt{\frac{2\Delta(v.e.)_{TR}}{m_{AV}}} = \sqrt{2}\quad U_{PCR1} \qquad (2)$$

Where:

$$\Delta(v.e.)_{TR} = \int_{T_{EXP}}^{T_R} C_p dT \qquad (3)$$

= Thermal vibratory energy per atom between T_{EXP} and T_R, Gram $(Cm/Sec)^2$.

C_P = Specific heat per atom as a function of temperature.

m_{AV} = Average mass of an atom in the material, Grams (Appendix A).

T_{EXP} = Temperature at which experimental impact shock tests are conducted. This is normally room temperature (RT≈ 300 ˚K but can (and should) be done at higher and lower temperatures.

T_R = Temperature at which some thermally induced reaction occurs (decomposition, melting, phase change, detonation, etc.).

U_{PCR2} = Particle velocity, U_P, such that the shock induced internal energy (e_i) is equal to $\Delta(v.e.)T_R$.

U_{PCR1} = Particle velocity, U_P, such that the total shock induced energy (e_t) (kinetic plus internal) is equal to $\Delta(v.e.)T_R$.

e_t = $m_{AV}U^2_P$ = total shock energy per average atom.

$e_i = \frac{m_{AV}}{2} U_p^2 = e_k =$ internal or kinetic energy of the shocked material per average atom.

Some explosives, when heated to higher and higher temperatures, melt before they explode (RDX and TNT, for example) This melting will require that the heat of fusion (ΔH_F) be absorbed by the material at $T=T_{MELT}$ conditions before the temperature will increase [13,14]. Consequently, if T_{EXP} is less than T_{MELT}, then the total heat absorbed from $T = T_{EXP}$ to $T = T_{EXPL} = T_R$ is:

$$\Delta (v.e.)_{T_R} = \int_{T_{EXP}}^{T_{MELT}} C_p dt + \Delta H_F + \int_{T_{MELT}}^{T_{EXPL}} C_p dT. \quad (4)$$

So, for solid energetic materials which melt prior to explosion, then $\Delta (v.e.)_{TR}$, as defined by Equation (4) is employed in Equations (1) and (2) to compute U_{PCR1} and U_{PCR2}, respectively. Note that melting is just one example of a phase transformation which may require an enthalpy increment (ΔH_T) to be activated. For example, HMX can exist in different solid polymorphic forms. At a certain temperature, T_T, one form may change to another form if the heat energy of transformation (ΔH_T) is supplied. So, ΔH_T should be added to Equations (3) and (4) if T_R is greater than T_T.

Note that $\Delta (v.e.)_{TR}$ as defined by Equations (3) and (4) is actually an enthalpy increment (ΔH). However, it was shown via numerical examples in Appendix B of Reference [1] that, under the experimental C_P acquisition conditions, the pressure times volume terms were minute compared to the C_P integral, $\int_{T_{EXP}}^{T_R} C_p dT$. Thus, $\int_{T_{EXP}}^{T_R} C_p dT$ is essentially all of the internal energy difference caused by thermal stimulation during standard tests at atmospheric pressure to determine the specific heat characteristics.

Once $\Delta (v.e.)_{TR}$ and U_{PCR} values are computed, the corresponding shock velocity (U_{SCR}) is ascertained from experimental data for U_S as a function of the particle velocity, U_P. The experimental relationship is usually linear and written empirically as:

$$U_S = C_O + S\, U_P. \quad (5)$$

Table 3 lists the constants, C_O and S and the data sources, for the explosives considered in this investigation.

When $U_P = U_{PCR}$ and $U_S = U_{SCR}$ are determined, the shock pressure is computed from the following well known relation:

$$P_S = \rho_o\, U_S U_P, \quad (6)$$

Where ρ_o = Material density (grams/cm^3).

Then U_{PCR} , U_{SCR} , and P_{SCR} may be compared to experimental shock-induced reaction threshold information to check the validity of the above Δ (v.e.)$_{TR}$ theory to denote reactive conditions under impact shock stimuli. The numerical computations involved in a Δ (v.e.)$_{TR}$ assessment are straightforward and simple and may be performed with a hand-held calculator.

It must be emphasized that any possible effect of pressure on C_P is not taken into account in the present analysis. The basic idea is that if a quantity of thermal vibration energy, Δ (v.e.)$_{TR}$, under quiescent conditions is able to create a reaction, then the same amount of energy added by an impact shock (e_i or e_t) should also cause some type of reaction. <u>The shock-induced reaction may not be the same type as the temperature induced reaction, but will nevertheless be a reaction of some kind.</u> It may be less or more severe than the thermally induced reaction.

The C_P unit of calorie/(atom - °K) is employed in plots of C_P versus T information which are shown in this report. This is because the Boltzman constant, k_B=0.33 x 10^{-23} calories/(atom - °K) and the maximum C_P at high temperatures for many materials is $3k_B \approx 1.0 \times 10^{-23}$ calories/(atom - °K). This is a good mnemonic reference level for comparison purposes. It was noted in Reference [1] that the average C_P per atom for most polymers never reaches the 3 k_B level before a reaction (phase change, melting, glass–to-rubber transition, or even detonation) occurs.

Actually, C_P for some atoms or combinations of atoms, probably reaches the 3 k_B level and causes a reaction at some T_R. But C_P for a large number of atoms remains much less than 2 k_B. Thus, a large amount of the possible thermal vibratory energy is never activated and the average C_P per atom remains relatively low [15]. In many cases, important temperature-induced reactions occur near the average $C_P \approx 2$ k_B level at moderate temperatures (400 to 600 °K).

It was shown in References [1] and [3] that the magnitude of the average C_P per atom at a given temperature for seven explosives did not differ very much from each other. The reaction temperatures, T_R, for these explosives did differ considerably, but m_{AV} values for these explosives were very similar. These observations, in conjunction with Equations (1) through (6), were sufficient to establish an overall correlation of experimental "shock sensitivity" data with reaction temperatures, T_R (primarily T_{MELT} and T_{EXPL}).

This report documents a similar correlation for PBX-9502 with T_{EXPL} at four different T_{EXP} conditions.

III. APPLICATIONS

Strictly speaking, for a valid check of the $\Delta(v.e.)_{TR}$ concept as outlined in Section II, the following experimental information is necessary for the <u>same</u> reactive energetic substance.

Thermal Properties:

1. Specific heat (C_P) as a function of temperature (T).
2. $T_R = T_{MELT}$ (melt), T_T (Transformation), T_{EXPL} (explode)
3. ΔH = Heat of fusion (ΔH_F, melt) and heat of transformation (ΔH_T).

Impact Shock Related Properties:

1. ρ_o, Material density (gram/cm^3) at each test condition temperature, T_{EXP}.
2. U_S (Shock velocity) as a function of particle or mass velocity (U_P) for each T_{EXP}.
3. Threshold U_{PDT} (or P_{SDT}), where below them detonation will not occur, and above them detonation will occur for each T_{EXP}.

It is rather difficult to find all of this consistent information for each T_{EXP}. In fact, it is unusual to locate impact shock results for a T_{EXP} other than RT ≈ 290 – 300°K).

However, there was one energetic material, PBX-9502, where impact shock-related data as described above, were available for four T_{EXP} conditions (-55 °C, RT, 75 °C, and 252 °C). Even so, some estimates, approximations, and extrapolations had to be made to fill in certain data gaps. This is particularly true for certain C_P data and the threshold U_P or P_S (for one T_{EXP} condition). Additional details of these data extension procedures are given in the following subsections.

A. PBX-9502 Experimental Thermal Data

Reference [10] contains experimental specific heat, C_P (Cal/Gram – °C), data in the temperature range of 37 °C (310 °K) to 177 °C (450 °K). These data had been fit to a straight line linear relation which could easily be extended backwards to T_{EXP} = -55 °C. Table 2 contains these data and also lists their values when converted to Cal/Atom – °C units.

Figure 1 compares this PBX-9502 and TATB C_P [Cal/(Atom – °C) data. As expected, C_P for these two materials does not differ very much in magnitude because PBX-9502 is 95 percent TATB. The TATB non-linear (quadratic fit) C_P data came primarily from Reference [5] with some extrapolation necessary at temperatures higher than 300 °C (573 °K). This estimated extension of the TATB C_P to 409 °C (682 °K) was essential to the $\Delta(v.e.)_{TR}$ analysis reported in References [1] and [2], and the present report as well. This was because some estimate of the PBX-9502 C_P was needed up to at least 396 °C (699 °K), which is given in Reference [12] as an explosion temperature (T_{EXPL}). To acquire this estimate, the linear relation for the C_P of PBX-9502 was extended from 177 °C (450 °K) to 292 °C (565 °K). From that point, the extended C_P for TATB was used for PBX-9502 also.

These C_P results (Cal/(atom –°C) for PBX-9502 are listed in Table 2 and displayed graphically in Figure 1. The cross-hatched areas shown below this PBX-9502 C_P versus T plot (between T_{EXP} and $T_R = T_{EXPL}$) are equal to $\Delta(\text{v.e.})_{TR}$ as defined by Equation (3).

The authors of Reference [12] heated PBX-9502 samples with a High Energy Electron Beam (HEEB) and provided the following information:

T_{EXPL}	=	Thermal explosion temperature
	=	396.0 $\pm$ 5.0 °C = 669.0 $\pm$ 5 °K
	=	Temperature at which the HEEB heating rate equals the chemical reaction rate.
TIT	=	Thermal ignition threshold
	=	140.0 $\pm$ 3.0 Cal./Gram
	=	Explosive heat dose
	=	Amount of thermal energy the energetic material can absorb before it explodes.

Reference [12] also gave T_{EXPL} = 409.0 $\pm$ 5.0 °C and TIT = 144.0 $\pm$ 5.0 Cal/Gram for TATB. The $\Delta(\text{v.e.})_{TR}$ results for TATB reported in Reference [1] for T_{EXP} = RT and $T_R = T_{EXPL}$ = 409 °C agreed well with this TIT value.

The extrapolations and assumptions involved in extending the PBX-9502 experimental C_P data to lower and higher temperatures detract somewhat from credibility, but appear reasonable compared to C_P data from other explosives. Also, as detailed later, a certain $\Delta(\text{v.e.})_{TR}$ value compares very well with the TIT value given above for PBX-9502. This lends considerable credence to the PBX-9502 extrapolations/extensions as $\Delta(\text{v.e})_{TR}$ is directly related to the C_P magnitude via Equation (3).

B. PBX-9502 Experimental 1-D Impact Shock Data

References [7] and [8] both document shock sensitivity (Hugoniot and run distance to detonation) experimental data for PBX-9502 at ambient room temperature (RT = $T_{EXP} \approx 12 - 27$ °C). In addition, Reference [8] also contains shock sensitivity results for PBX-9502, which was collected at -55 °C, 75 °C, and 252 °C. These investigators illustrated shock sensitivity to test temperatures by comparing run-distance-to-detonation (X_D) versus shock pressure (P_S) data on double-log Popalato (POP) plots. Most of these data are also graphically displayed in Reference [6].

From these sources, the following information was extracted which was essential to the present analysis where detonation threshold particle velocities (U_{PDT}) were compared to theoretical U_{PCR} results defined in Section II:

a. ρ_o (Density, grams per cubic centimeter) as a function of temperature, T_{EXP}. These ρ_o values are listed in Tables 3 and 5.

b. U_S (Shock Front Velocity) as a function of U_P (particle or mass velocity) generated in the PBX-9502 specimen for each T_{EXP}. The pertinent values of C_O and S, for Equation (5), are listed in Table 3.

c. Threshold U_{PDT} values, just sufficient to cause detonation, were determined from tabular or graphical (POP plots) data for P_S (or U_P) as a function of run-distance-to-detonation, X_D, contained in References [6, 7, and 8].

The procedure to determine the threshold U_{PDT} values is illustrated in Figures 2 through 5, where U_P versus X_D is plotted on a linear scale from the tabulated/plotted data in References [6], [7], and [8].

For T_{EXP} = RT, 75 °C, and 252 °C, tabulated U_P versus X_D experimental data asymptotically approach a practical detonation threshold value of U_{PDT} as X_D gets larger and larger as shown in Figures 3, 4, and 5, respectively.

The values estimated by this procedure are 0.88, 0.82, and 0.46 km/sec for T_{EXP} = RT, 75 °C and 252 °C, respectively. These estimated U_{PDT} threshold values also appear reasonable as shown in Figures 6, 7, and 8, where U_P is plotted versus t_D (time to detonation) for T_{EXP} = RT, 75 °C and 252 °C, respectively.

The U_S versus U_p variation for PBX-9502 at RT conditions indicates some type of impact-induced reaction is occurring around $U_p = 1.0 \pm 0.2$ km/sec where a slope (dU_S/dU_p) change is evident [7, 20]. This is consistent with the RT U_{PDT} estimated result of 0.88 km/sec.

The estimation of the detonation threshold U_{PDT} for T_{EXP} = - 55 °C was not quite so straightforward as that for T_{EXP} = RT, 75 °C, and 252 °C. The reasons for this are detailed as follows.

The shock sensitivity data (Ps, X_D) from PBX-9502 experiments at T_{EXP} = -55 °C were apparently documented in Reference [9]. References [6] and [8] show these results in the form of X_D versus P_S points on a double-log POP plot. For most explosives, X_D versus P_S is a linear (straight line) function on a log-log POP plot. This seems to be true for PBX-9502 at -55 °C and LX-17 at ambient (RT) conditions, which both exhibit the same trend (slope) and magnitude.

However, the PBX-9502 data plot at -55 °C began at $X_D \approx$ 10mm with a corresponding P_S of about 140 kbars. This is obviously somewhat different from the threshold values for this condition. A linear extrapolation back to $X_D \approx$ 50.0 mm gives a P_S value of about 90.0 kbars, which should be close to the threshold (go or no go) value. The corresponding result of U_{PDT} is 0.95 km/sec, which is found via Equations (5) and (6) with the appropriate input conditions.

Table 4 gives a list of the X_D versus P_S points extracted from the PBX-9502 data for T_{EXP} = -55 °C, shown in Figure IV-9 of Reference [6]. The corresponding values of U_P are also listed in this table. They are plotted versus X_D in Figure 2 of the present report where an extrapolation is made to yield a threshold value of U_{PDT} equal to around 0.94 or 0.95 km/sec for this T_{EXP} condition.

All of this extrapolation to estimate this detonation threshold U_{PDT} value at T_{EXP} = -55 °C detracts from credibility, but the result seems reasonable (with the proper trend and magnitude) as shown in Figure 9.

Figure 9 depicts the estimated detonation threshold U_{PDT} values versus T_{EXP}. These results are also listed in Table 5. It is these U_{PDT} results (determined basically from experimental data) that the computed U_{PCR1} and U_{PCR2} are compared with in order to check the validity of the $\Delta(v.e.)_{TR}$ concept.

$\Delta(v.e.)_{TR}$ magnitudes (and thus U_{PCR1} and U_{PCR2} magnitudes) also depend entirely on experimental information (C_P vs. T and T_R). Therefore, a check on the validity of the $\Delta(v.e.)_{TR}$ concept is essentially a check on the consistency of the experimental thermal and impact shock data.

C. PBX-9502 $\Delta(v.e.)_{TR}$, U_{PCR}, and P_{SCR} Results

This subsection delineates the combination of information from both A and B sub-sections to systematically compute $\Delta(v.e.)_{TR}$, U_{PCR}, and P_{SCR} results for each experimental test condition (T_{EXP}) with a plausible reactive temperature (T_R) value.

Basically, $\Delta(v.e.)_{TR}$ was computed via numerical integration of the area under the PBX-9502 C_P versus T Data Plot (Fig. 1) between T_{EXP} and T_R. These areas were either trapezoids or rectangles because the C_P variation with T was linear or constant as discussed above.

$\Delta(v.e.)_{TR}$ was evaluated for each of the four temperatures (-55 °C, RT, 75 °C and 252 °C) where experiments were conducted. This was done for only one reactive temperature ($T_R = T_{EXPL}$ = 396 °C = 669 °K) given in Reference [12] as the temperature where an explosion occurred under the rapid heating from a HEEB.

PBX-9502 can explode at lower temperatures, particularly if soaked for a long period of time (14 hours) at a constant temperature just above the so called Arrhenius critical temperature. This is T_{CR} = 296 °C = 542 °K which is described in Reference [11] as:

> "That surface temperature at which the internal energy generated by chemical decomposition is greater than that which can be removed through the surface by thermal conduction."

If soaked at a temperature below T_{CR}, apparently no explosion occurs. T_{CR} = 296 °C = 542 °K was not employed as a reactive temperature, T_R, in the present analysis because the time scales involved in these so called Arrhenius tests (hours) and impact shock loading (µsec) are vastly different. The rapid heating (energy input) during HEEB tests [12] is much more compatible to impact shock loading energy deposition conditions than slow cook-off tests.

Thus, $T_R = T_{EXPL}$ = 396 °C = 669 °K from the HEEB tests [12] was employed for the $\Delta(v.e.)_{TR}$ computations.

Table 6 lists the $\Delta(v.e.)_{TR}$ values computed for each of the four temperatures (T_{EXP}) where impact shock experiments were conducted. Table 6 also lists the associated results for U_{PCR1} and U_{PCR2}. Table 7 lists the corresponding U_{SCR} and P_{SCR} information.

U_{PCR1} and U_{PCR2} are plotted versus T_{EXP} in Figure 9 where, for comparative purposes, the estimated detonation threshold, U_{PDT}, results are also shown.

IV. DISCUSSION

Reference [8], in particular, illustrated PBX-9502 impact shock sensitivity to different test condition temperatures (T_{EXP}). This was accomplished via impact testing at different temperatures and the results were presented in POP plots (X_D vs. P_S) from Figure 5 in Reference [8]. There are both amplitude and slope changes which illustrate impact shock sensitivity to temperature. For instance, PBX-9502 at T_{EXP} = -55 °C and +75 °C are slightly above and below, respectively, the POP plot for ambient RT conditions. So, there was not a large change in shock sensitivity at T_{EXP} = -55 °C and +75 °C (compared to T_{EXP} = RT), but there was a large change (increased shock sensitivity) for T_{EXP} = 252 °C.

This report attempts to provide a quantitative explanation for the temperature-related impact sensitivity phenomena described above. These trends are in agreement with the detonation threshold U_{PDT} data (Section III-B) listed in Table 5 and depicted versus T_{EXP} in Figure 9. This is, perhaps, to be expected because the U_{PDT} results were derived from the same experimental POP plot data.

There is not much difference in:

$U_{PDT} = 0.94$	km/sec	T_{EXP} = -55 °C
$U_{PDT} = 0.88$	km/sec	T_{EXP} = RT
$U_{PDT} = 0.82$	km/sec	T_{EXP} = 75 °C

There is only 0.06 km/sec difference in U_{PDT} for ambient RT and U_{PDT} for T_{EXP} = -55 °C and U_{PDT} for T_{EXP} = 75 °C.

This same trend shows up in the computed results for U_{PCR1} and U_{PCR2} at T_{EXP} = -55 °C, RT and 75 °C. Fundamentally, there is just not that much difference between $\int_{T_{EXP}}^{T_R} C_P dT = \Delta(\text{v.e.})_{TR}$ for these conditions, as shown in Table 7. U_{PCR} is proportional to the square root of $\Delta(\text{v.e.})_{TR}$ which makes the differences in U_{PCR} even less.

When T_{EXP} = 252°, this is much closer to T_R = 396 °C than T_{EXP} for the other three test conditions. The value of $\int_{252}^{396} C_P dT = \Delta(\text{v.e.})_{TR}$ for this case is less than half of $\Delta(\text{v.e.})_{TR}$ for the other three test conditions (Table 7). Consequently, the U_{PCR} values for T_{EXP} = 252 °C are considerably less than U_{PCR} results for the other three test cases at lower temperatures. This is because much more heat energy had been added to the explosive target before it was impact shock loaded. This is consistent with the experimental U_{PDT} results for this test case (Table 5 and Fig. 9).

It should be noted that T_R = 396 °C for PBX-9502 is rather large compared to most explosives [1 and 3]. For T_R values much less than this, these explosives will exhibit more variation in impact shock loading sensitivity at temperatures closer to ambient RT (say -55 ° or 75 ° C) than PBX-9502. This follows from the integral limits (T_{EXP} and T_R) in the definition of $\Delta(\text{v.e.})_{TR}$.

One highly affirmative check on the $\Delta(\text{v.e.})_{TR}$ computations with T_{EXP} = RT (20 °C) and T_R = 396 °C is as follows for these PBX-9502 conditions:

$\Delta(\text{v.e.})_{TR}$ = 247.8165(10^{-23}) calories per average atom (Table 6).

= 136.0747 cal/gram because m_{AV} = 1.82118(10^{-23}) grams per average atom of PBX-9502.

This compares rather well with:

TIT = 140.0 +/- 3.0 cal/gram

= thermal ignition threshold from HEEB tests (see Section III.A and Reference [12]).

This is certainly indicative of reasonably good values of C_P versus T information for the $\Delta(\text{v.e.})_{TR}$ computation at this condition. No adjustments to the C_P versus T information were made in order to yield this good comparison between these $\Delta(\text{v.e.})_{TR}$ and TIT values.

V. CONCLUSIONS

Based on the good comparative results described in the preceding section and the previous work, documented in References [1] through [4], it is concluded that the $\Delta(v.e.)_{TR}$ concept for explosives:

1. Provides a quantitative connection between impact shock sensitivity (U_{PDT} or P_{SDT}) and the thermal properties (C_P and T_R).

2. Illustrates the consistency between experimental impact shock results and the thermal properties.

3. Provides additional support for the premise that the specific heat per average atom (at a given temperature up to T_R) has approximately the same magnitude. See References [1] through [4] where this is illustrated for several important secondary CHNO energetic materials.

4. Indicates that high reactive temperatures (T_R) are related to phenomenal impact shock insensitivity such as exhibited by TATB and PRX-9502. That is, as T_R becomes larger, higher impact shock pressure (P_S), or actually larger particle velocity (U_P), is required to initiate detonation. This is quantitatively explained by Paragraph 3 above and the basic definition of $\Delta(v.e.)_{TR}$ that is Equation (3) where the upper limit of the integral is T_R. As T_R increases, so does $\Delta(v.e.)_{TR}$ which is the amount of heat energy (or impact shock energy) that can be absorbed before a reaction occurs.

VI. RECOMMENDATIONS

In order to perform this comparative analysis, the amount of experimental data extrapolation and judicious extension necessary to provide certain impact shock and thermal information suggests that:

1. Experimental C_P versus T data should be collected for as wide a range of T as possible on both sides of ambient (RT) conditions.

2. Plane impact shock detonation thresholds (U_{PDT} of P_{SDT}) should be delineated at each temperature (T_{EXP}) where these experiments are conducted.

3. Along with recommendation No. 2, U_S versus U_P data are also needed at each T_{EXP} in order to compute U_{SCR} and P_{SCR} from the U_{PCR} results.

These are generalizations of the specific recommendations made in Reference [1]. They apply, of course, to present explosives, but are particularly relevant to new explosives under development.

It is realized that these recommendations may be difficult, or practically impossible, to perform, particularly at high temperatures where a violent reaction may occur.

One other recommendation, or admonishment, to impact shock investigators is:

> Pay as much attention to particle (or mass) velocity (U_P) magnitudes as a measure of shock induced reactions as is currently bestowed on shock pressure (P_S) levels.

This advice is solidly based on the investigations documented in References [1] through [4] and this report, plus additional studies concerning other shock loading induced reactions of solid materials not cited herein.

Table 1. Thermal Properties of TBX-9502

Property	Reference	Value
T_{EXPL} Thermal Explosion Temperature	[12]	396.0 +/- 5.0 °C 669.0 +/- 5.0 °K
TIT Thermal Ignition Threshold	[12]	140.0 +/- 3.0 Cal/Gram
Δ H_F Heat of Fusion	[11]	50.0 Cal/Gram at 420.0 °C (693 °K)
C_P Specific Heat	[5, 6, 10]	See Table 2.
T_{CR} (See IIIC for Definition)	[6] [11]	344.3 ˚C to 356.0 ˚C 617.3 ˚K to 629.0 ˚K 269.0 °C 542.0 °K

Table 2. PBX – 9502 Specific Heat (C_P)

T	T	0.00059T(°C)	C_P	C_P	Comments
°C	°K	CAL/(Gram-°C)	CAL/(Gram-°C)	CAL/(Atom-°C)	~ ~ ~ ~ ~ ~
-55*	218*	-0.03245	0.21655	0.39438 * 10-23	PBX – 9502 Linear Extrapolation
0	273	0.0	0.24900	0.45347 * 10-23	
17	290	0.01003	0.25903	0.47174 * 10-23	
20*	293*	0.01180	0.26080	0.47496 * 10-23	
27	300	0.01593	0.26493	0.48249 * 10-23	
37	310	0.02183	0.27083	0.49323 * 10-23	PBX – 9502 Test Data ***
75*	348*	0.04425	0.29325	0.53406 * 10-23	
100	373	0.05900	0.30800	0.56090 * 10-23	
177	450	0.10443	0.35340	0.64370 * 10-23	
227	500	0.13393	0.38290	0.69730 * 10-23	PBX – 9502 Linear Extrapolation
252*	525*	0.14868	0.39770	0.72420 * 10-23	
275	548	0.16225	0.41125	0.74896 * 10-23	
280	553	0.16520	0.41420	0.75433 * 10-23	
300	573	~	~	0.75910 * 10-23	←End of TATB Data
396**	669**	~	~	0.75910 * 10-23	← TATB Data Extrapolation

* T = T_{EXP} (Experimental Test Condition, [8])

** T = T_{EXPL} (PBX – 9502 Explosion Temperature [12])

*** PBX – 9502 $C_P = 0.249 + 0.00059T$ (°C) for 37 °C ≤ T ≤ 177 °C, Ref. [10]

PBX – 9502 $m_{AV} = 1.82118 * 10^{-23}$ Grams/Atom

Table 3. Impact Shock Loaded Material Data for $U_S = C_O + S\ U_P$ Relation

Material	TEXP	ρ_O	C_O	S	Source	Remarks
~	°C	Grams	KM	~	~	~ ~ ~ ~ ~ ~ ~ ~
	°K	CM3	SEC			
↓	↓					
↓	-55 °C	1.91	3.31	1.65	[8]	See Figure 6 in [8].
PBX-9502	218 °K					
↑	↑					
↓	↓					
↓	20 ± 8 °C	1.891	1.857	3.15	[7]	$U_P \leq 0.50$ KM/SEC
↓	293 ± 8 °K					
↓	↓					
↓	↓		Non-Linear See Remarks & Fig. 4 in [7]			$U_S = 1.392201 + 5.153578\ U_P$
↓	RT				[7]	$-2.421567\ U_P^2$ $+0.561615\ U_P^3$
↓	↑					For $0.5 < U_P < 1.2$ KM/SEC
↓	↑					
↓	↑		2.938	1.77	[7]	$1.2 \leq U_P < 2.3$ KM/SEC
↓	↓					
↓	RT	1.891	1.90	3.00	[20]	$U_P \leq .082$ km/sec
↓	↓	1.891	2.90	1.78	[20]	$U_P \geq 0.82$ km/sec
↓	75 ± 2 °C	1.857	2.60	1.91	[8]	See Figure 6 in [8].
↓	348 ± 2 °K					
↓	↑					
↓	↓					
↓	252 ± 2 °C	1.70	1.33	3.08	[8]	See Figure 6 in [8].
↓	525 ± 2 °K					
↓	↑					

Table 4. PBX-9502 U_P Versus X_D Information From Popolato Plots in References [6] and [8] for T_{EXP} = -55 °C = 218 °K

	X_D [6,8]	P_S [6,8]	Comment	ρ_O	U_P	U_S	P_S
	MM	KBAR		GRAM/CC	KM/SEC	KM/SEC	KBAR
	1.4	250.0	Note 1	1.91	2.00	6.6100	252.50
	2.0	230.0	↓	↓	1.88	6.4120	230.24
	3.0	205.0	↓	↓	1.74	6.1810	205.42
	7.0	160.0	↓	↓	1.47	5.7355	161.04
	10.0	140.0	↓	↓	1.33	5.5045	139.83
	18.0	120.0	Note 2	↓	1.19	5.2735	119.86
	30.0	105.0	↓	↓	1.08	5.0920	105.04
	40.0	95.0	↓	↓	1.00	4.9600	94.74
	50.0	89.0	↓	↓	0.95	4.8775	88.50
	>50.0	89.0	↓	↓	0.94	4.8610	87.27

Note 1. From Figure IV-9 in [6].

Note 2. Linear Extrapolation

Note 3. $U_s = 3.31 + 1.65U_p$

Note 4. $P_S = \rho_O U_S U_P$

Table 5. PBX-9502 Estimated Impact Shock Induced Threshold Information
From U_P, $V_{S,}$ X_D Data

T_{EXP}	T_{EXP}	X_D	Up_{DT}	Us_{DT}	Ps_{DT}	ρ_o			Comments		
°C	°K	MM	KM/SEC	KM/SEC	KBA R	GR/CC		~	~	~	~
-55	218	≈50.0 >50.0	0.95 0.94	4.8775 4.8610	88.50 87.27	1.91			See Figure 2.		
12 – 28 (RT)	285–301 (RT)	≈40.0 39.9	0.88 0.88	4.4348 4.46 EXP.	73.92 74.80 EXP.	1.891			See Figures 3 & 6.		
75	348	≈40.0	0.82	4.1662	63.44	1.857			See Figures 4 & 7.		
252	525	≈40.0	0.46	2.7468	21.48	1.70			See Figures 5 & 8.		

Table 6. Computation of Up_{CR1} and Up_{CR2}

ITEM ~	m_{AV}	T_{EXP}	T_R	Remarks	$\int_{T_{EXP}}^{T_R} C_p dT$	$\int_{T_{EXP}}^{T_R} C_p dT$	$\int_{T_{EXP}}^{T_R} C_p dT$	ΔH_T	$\Delta(v.e.)_{TR}$	$\frac{\Delta(v.e.)_{TR}}{m_{AV}}$	Up_{CR1}	Up_{CR2}
~	Grams $*10^{-23}$	°C °K	°C °K	~	Cals $*10^{-23}$	Joules $*10^{-23}$	$G(Cm/Sec)^2$ $*10^{-13}$	$G(Cm/Sec)^2$ $*10^{-13}$	$G(Cm/Sec)^2$ $*10^{-13}$	$(Cm/Sec)^2$ $*10^{+10}$	Km/Sec	Km/Sec
PBX-9502	1.82118	-55 218	396 669 (T_{EXPL})	No ΔH	280.4168	1,173.264	1.173264	0.00	1.173264	0.64423	0.8026	1.1351
PBX-9502	1.82118	20 293 RT	396 669 (T_{EXPL})	No ΔH	247.8165	1,036.864	1.036864	0.00	1.036864	0.56933	0.7545	1.0671
PBX-9502	1.82118	75 348	396 669 (T_{EXPL})	No ΔH	220.0683	920.7658	0.9207658	0.00	0.9207658	0.50559	0.7110	1.0056
PBX-9502	1.82118	252 525	396 669 (T_{EXPL})	No ΔH	108.7080	454.8343	0.4548343	0.00	0.4548343	0.24975	0.4997	0.7067

Table 7. Computation of Us_{CR} and Ps_{CR}

ITEM ~	T_{EXP} °C ° K	ρ_O Grams/Cm^3	C_O Km/Sec	S ~	Remarks	Up_{CR1} Km/Sec	Us_{CR1} Km/Sec	Ps_{CR1} Kbars	T_R °C ° K	Up_{CR2} Km/Sec	Us_{CR2} Km/Sec	Ps_{CR2} Kbars
PBX-9502	-55 218	1.910	3.31	1.65	No ΔH	0.8026	4.6343	71.042	396 669 (T_{EXPL})	1.1351	5.1351	112.368
PBX-9502	20 293 (RT)	1.891	Non - Linear See Table 3.		No ΔH	0.7545	4.1433	59.115	396 669 (T_{EXPL})	1.0671	4.8166	97.193
PBX-9502	75 348	1.857	2.60	1.91	No ΔH	0.7110	3.9580	52.259	396 669 (T_{EXPL})	1.0056	4.5207	84.419
PBX-9502	252 525	1.700	1.33	3.08	No ΔH	0.4997	2.8691	24.373	396 669 (T_{EXPL})	0.7067	3.5066	42.128

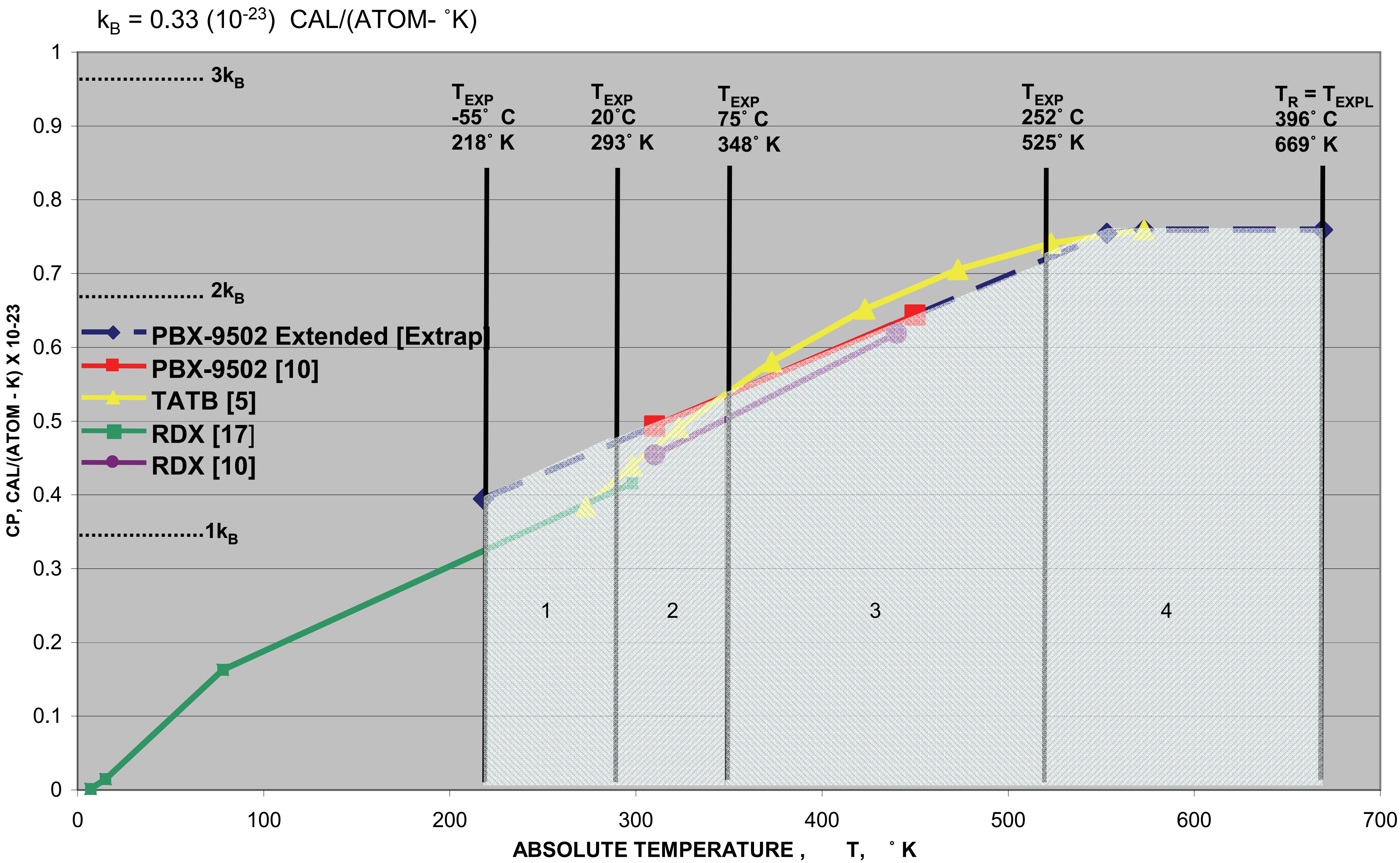

Figure 1. Specific Heat per Average Atom for PBX-9502, TATB, and RDX

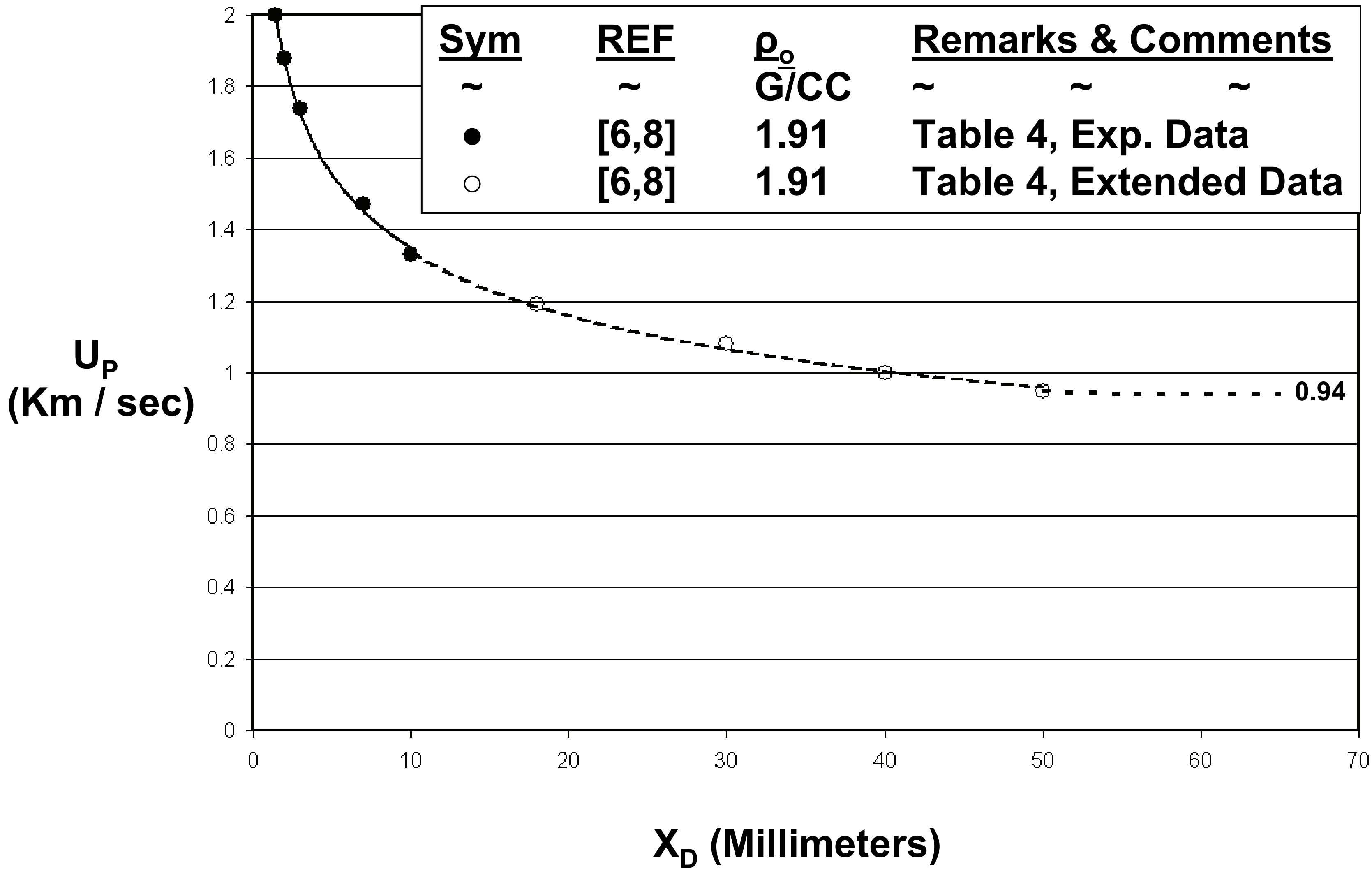

Figure 2. U_P Versus X_D for PBX-9502 at T_{EXP} = - 55 ºC = 218 ºK

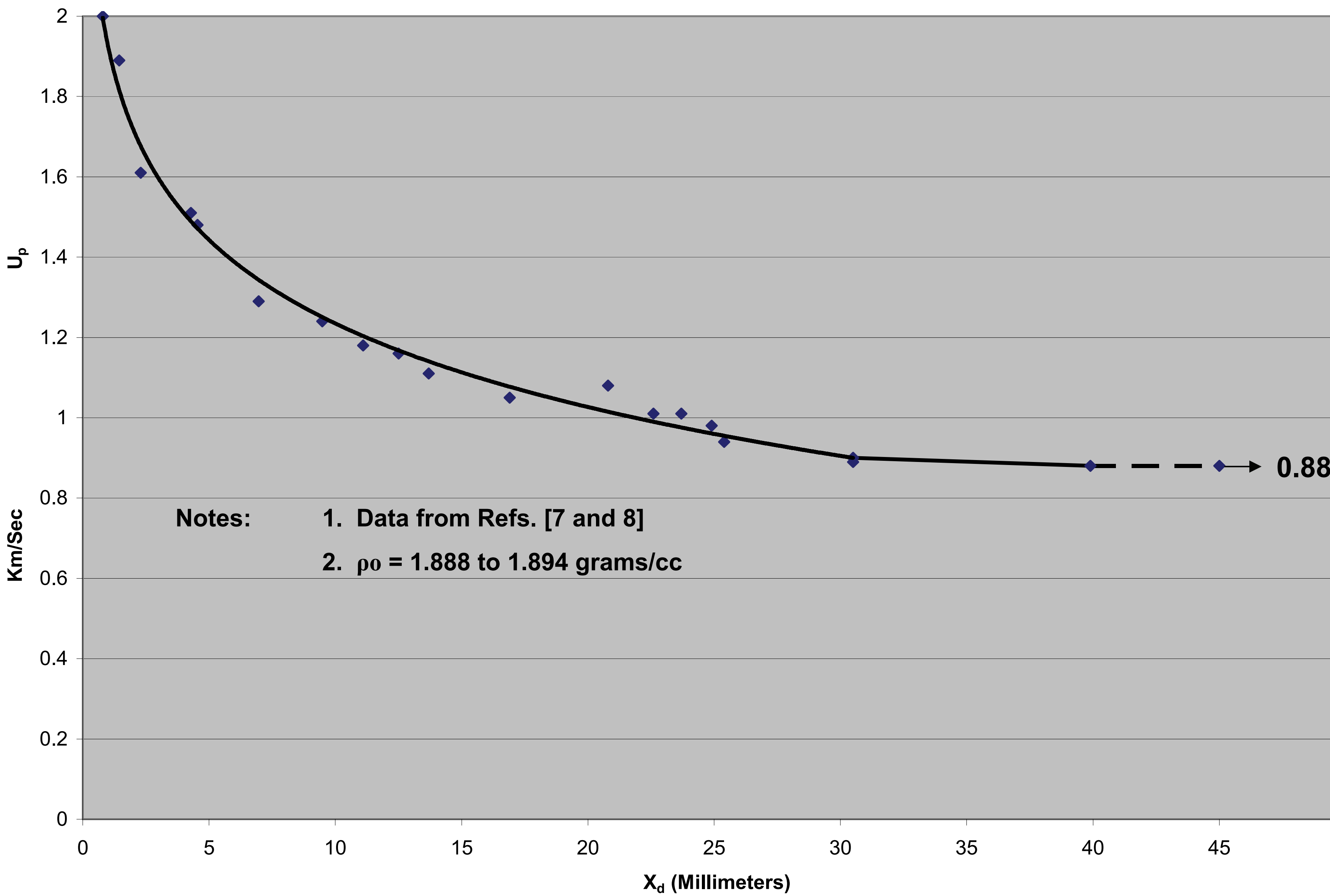

Figure 3. U_p Versus X_D for PBX-9502 at T_{EXP} = Ambient Room Temperature (R T)

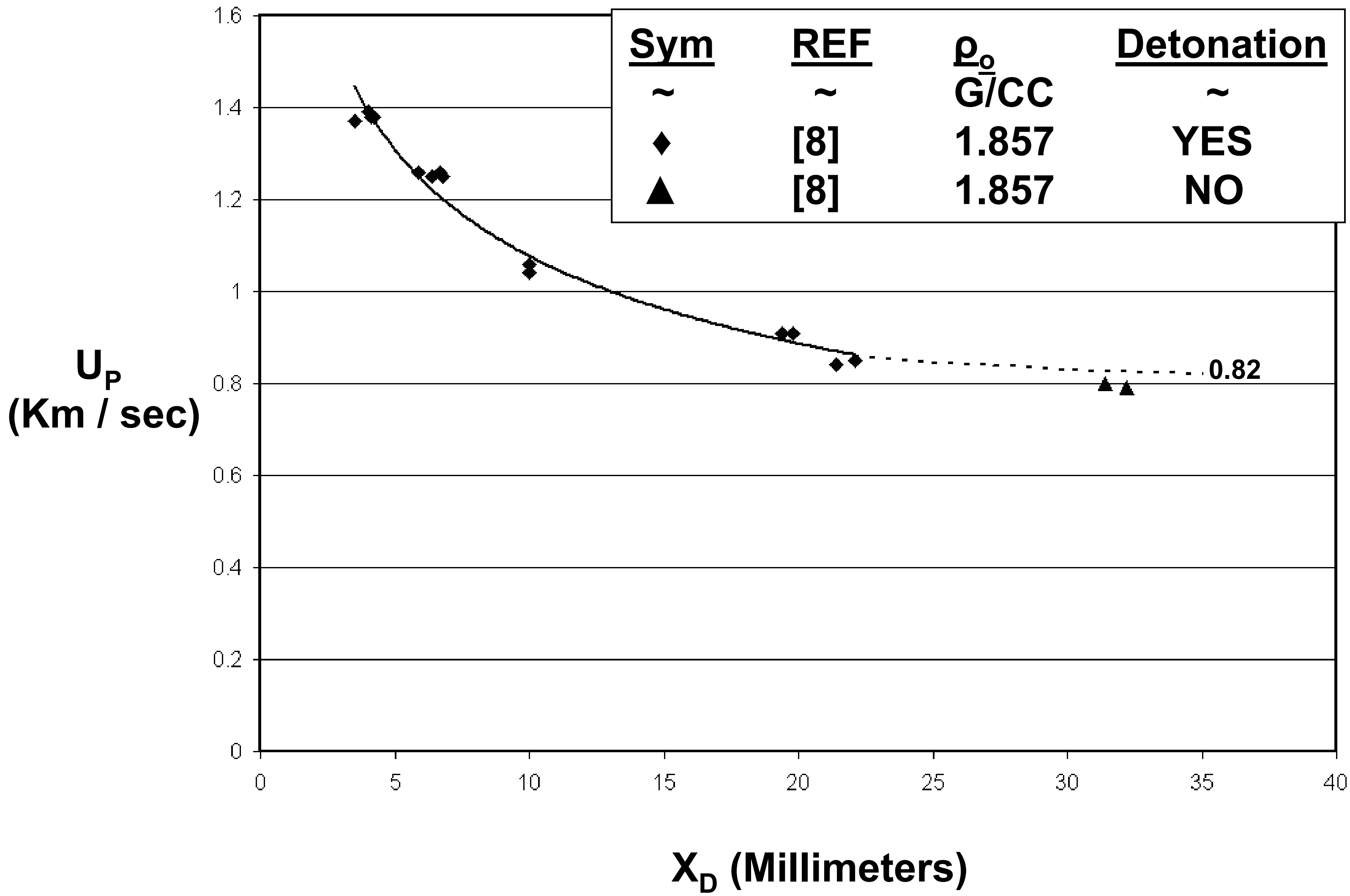

Figure 4. U_P Versus X_D for PBX-9502 at T_{EXP} = 75 ºC = 348 ºK

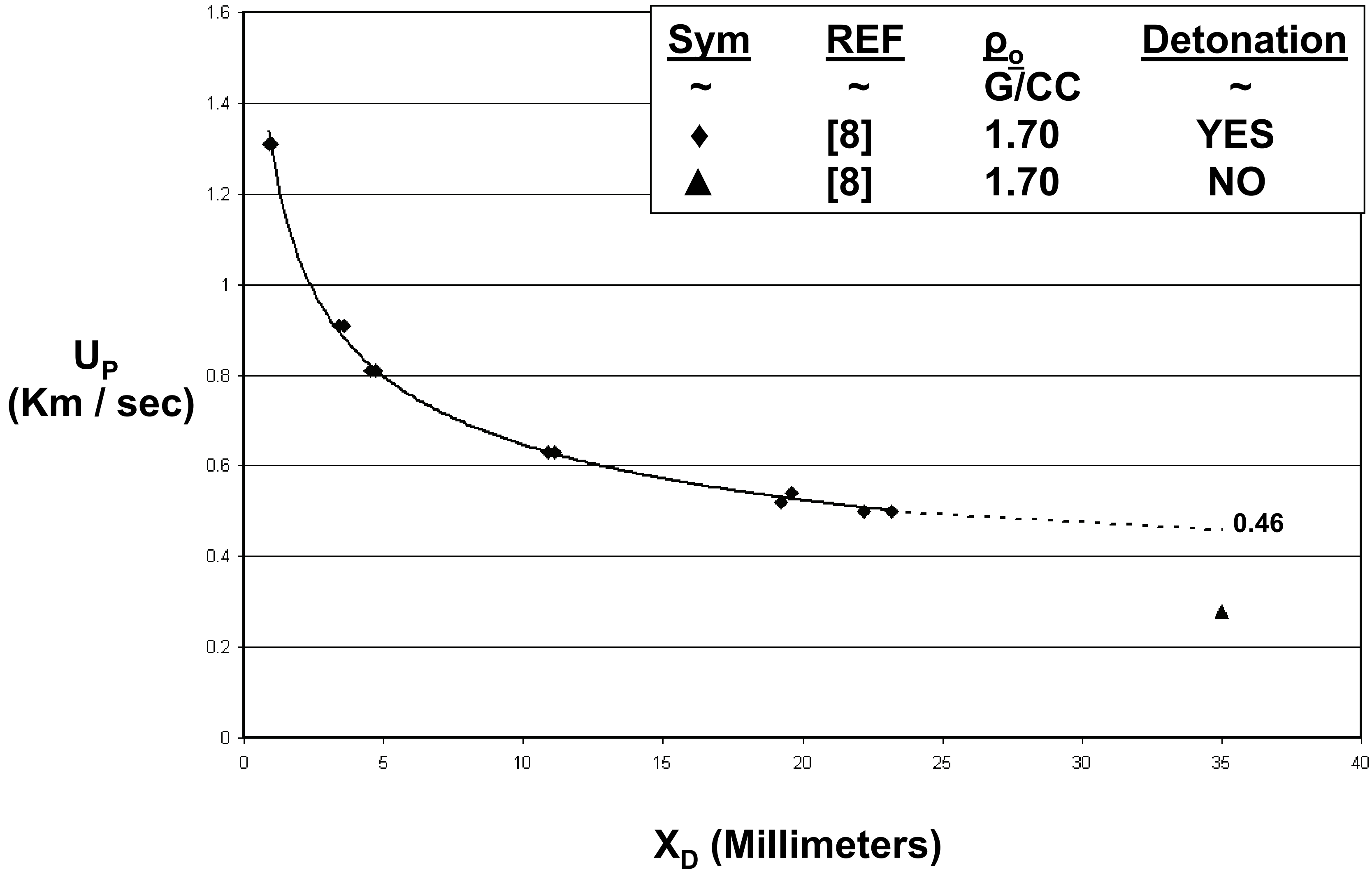

Figure 5. U_P Versus X_D for PBX-9502 at T_{EXP} = 252 ºC = 525 ºK

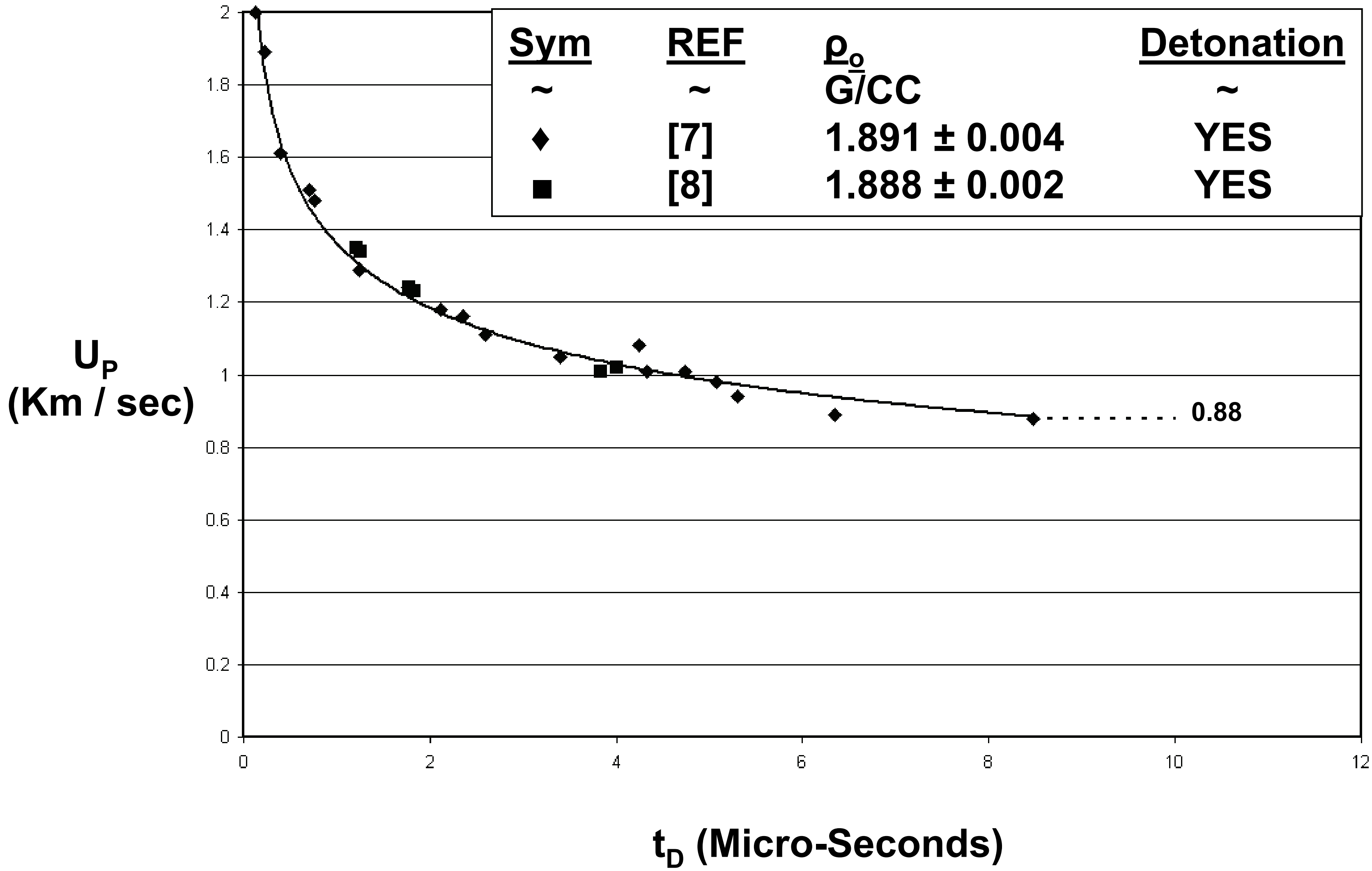

Figure 6. U_P *Versus* t_D *for PBX-9502 at* T_{EXP} *= RT Conditions*

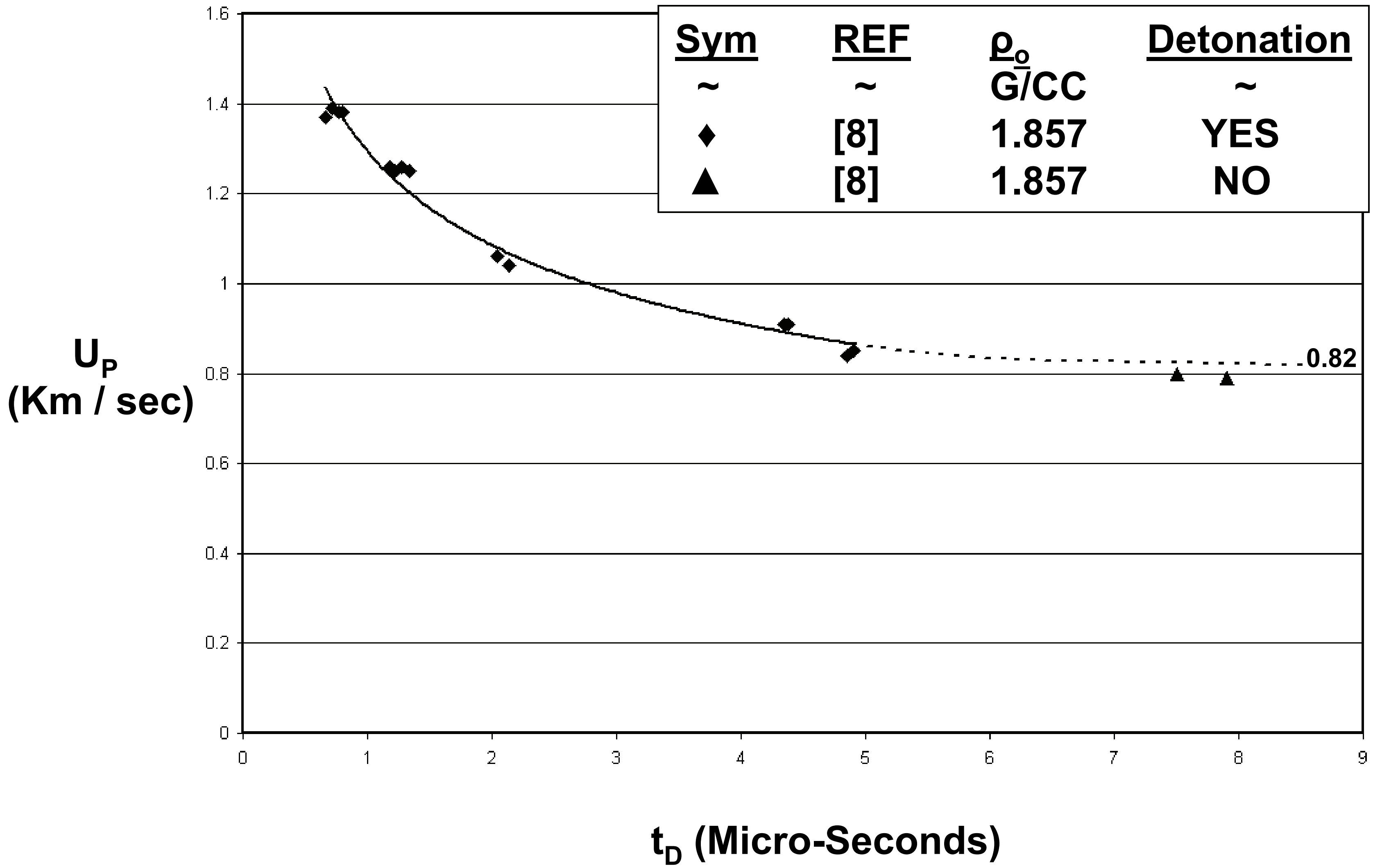

Figure 7. U_P Versus t_D for PBX-9502 at T_{EXP} = 75 ºC = 348 ºK

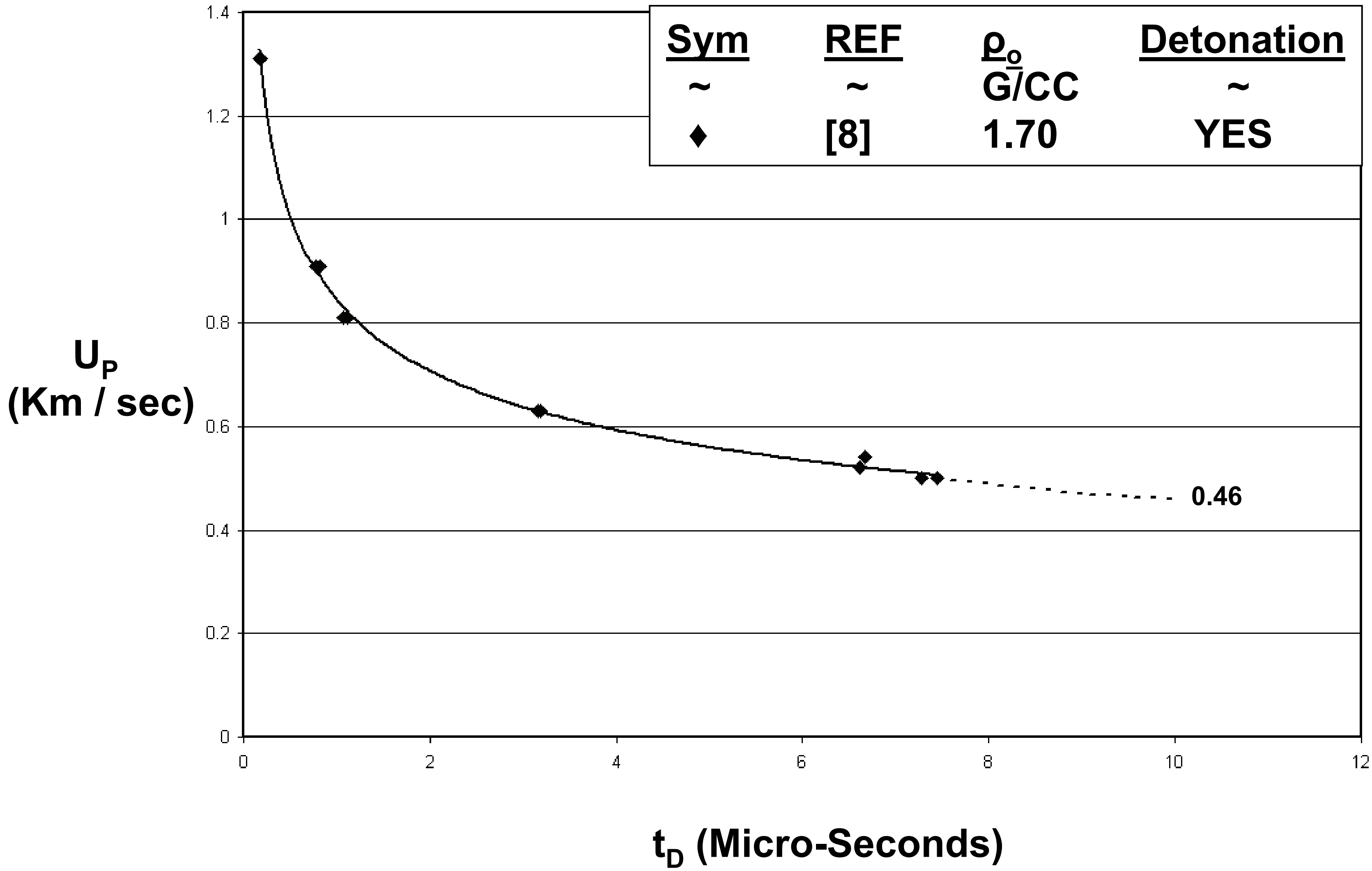

Figure 8. U_P Versus t_D for PBX-9502 at T_{EXP} = 252 ºC = 525 ºK

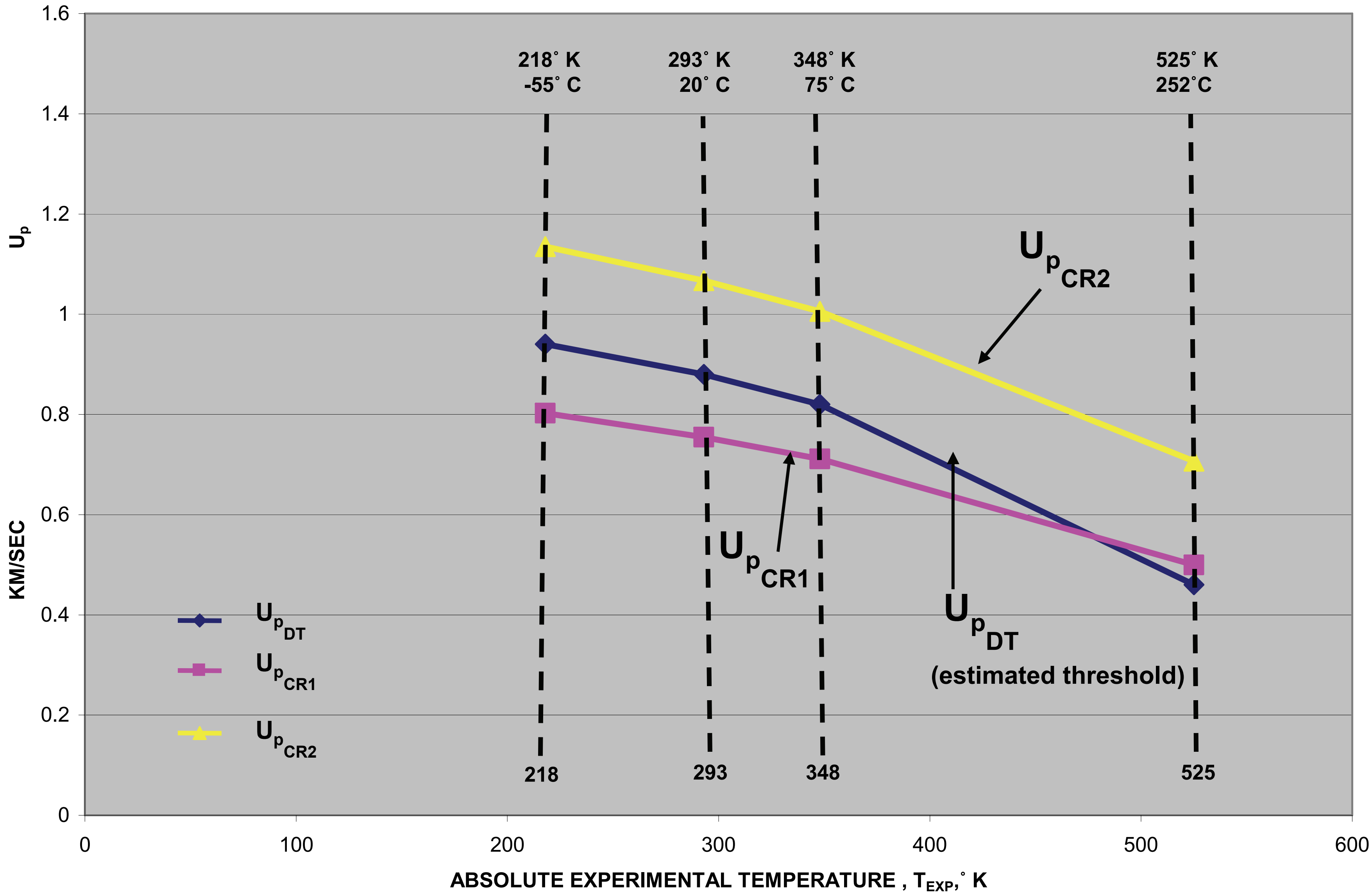

Figure 9. Detonation Threshold ($U_{P_{DT}}$) and Theoretical ($U_{P_{CR}}$, No ΔH_F) Results for PBX-9502, T_R = 396 ˚C = 669 ˚K = T_{EXPL}

REFERENCES

1. Billingsley, J. P., “Energetic Materials Shock Sensitivity Relevance to Specific Heat Properties.” Technical Report RD-SS-95-2, July 1995, U.S. Army Missile Command, Redstone Arsenal, Alabama, 35898.

2. Billingsley, J. P., “Energetic Materials Shock Sensitivity Relevance to Specific Heat Properties,” Paper in Shock Compression of Condensed Matter – 1995, AIP Conference Proceedings, 370, Part 1, Pages 429-432.

3. Billingsley, J. P., “Two Additional Examples of Energetic Materials Shock Sensitivity Correlations with Specific Heat Characteristics,” Technical Report RD-SS-99-8, June 1999, U.S. Army Missile Command, Redstone Arsenal, Alabama, 35898.

4. Billingsley, J. P., “HMX and HNS Shock Sensitivity Correlation with Specific Heat and Reactive Temperature Magnitudes,” Paper in Shock Compression of Condensed Matter – 1999, AIP Conference Proceedings 505, Part II, Pages 899-902.

5. Dobratz, B. M., “LLNL Explosives Handbook, Properties Handbook, Properties of Chemical Explosives and Explosives Simulants,” Report UCRL-52997, March 16, 1981, Lawrence Livermore Laboratory, University of California, Livermore, CA 94550.

6. Dobratz, B. M., “The Insensitive High Explosive Triamino Trinitro Benzene (TATB): Development and Characterization – 1888-1994,” Los Alamos National Laboratory Report LA-13014-H, UC-741, August, 1995.

7. Dick, J. J.; Forest, C. A.; Ramsey, J. P.; and Seitz, W. L., “The Hugoniot and Shock Sensitivity of a Plastic Bonded TATB Explosive PBX-9502,” Journal of Applied Physics, Vol. 63, No. 10, 15 May 1988, Pages 4881-4888.

8. Dallman, J. C., and Wackerle, J., “Temperature-Dependent Shock Ignition of TATB-Based High Explosives.” Paper in Proceedings of the Tenth International Detonation Symposium, July 12-16, 1993, Published as an Office of Naval Research Report, ONR-33345-12, Pages 130-138.

9. Seitz, W. L., and Wackerle, J., “Prompt Initiation Studies of PBX-9502 and PBX-9503.” The Fifth Annual Joint Firing System Conference (LFSC/XUSC) (Oct. 1980).

10. Baytos, John F., “Specific Heat and Thermal Conductivity of Explosives, Mixtures, and Plastic-Bonded Explosives Determined Experimentally.” Los Alamos National Laboratory, Los Alamos, NM, LA-8034-MS (1979).

11. Jaeger, D. L., “Thermal Response of Spherical Explosive Charges Subjected to External Heating,” LA-8332, UC-45, Aug, 1980, Los Alamos Scientific Laboratory Report.

REFERENCES (CONT)

12. Stolovy, A.; Aviles, J. B.; Jones, E. C. Jr.; and Namenson, A. I., “Electron Beam Initiation of High Explosives”, Seventh International Symposium of Detonation Proceedings, June 16-19, 1981, Published as NSWC MP 82-334, Pages 50-55.

13. Black, N. H., An Introductory Course in College Physics. The MacMillan Company, New York, 1950, pp. 270-274/

14. Stull, D. R.; Westrom, E. F. Jr.; and Sinke, G. C., The Chemical Thermodynamics of Organic Compounds, John Wiley and Sons, Inc., New York, 1996.

15. Van Krevelen, D. W., and Hoftyzer, P. J., Properties of Polymers, Elsevier Scientific Publishing Company, Amsterdam, 1976.

16. Urtiew, P. A.; Cook, T. M.; Maienschein, J. L.; and Tarver, C. M., “Shock Sensitivity of IHE at Elevated Temperatures”. Paper in Tenth International Detonation Symposium Proceedings, Published as ONR 33395-12, July 12-16, 1993, Pages 139-147.

17. Rey-Lefon, Madeline, and Bonjour, Emmanuel, “Etude de la Chaleur Specifique de la Trinitro-1, 3, 5, Hexahydro-s-triazin Cristallissee. Determination Experimentale et Calcul a Partir des Frequences de Vibration Infrarouges et Raman”. Molecular Crystals and Liquid Crystals, Vol. 24 pp. 191-199 (1973).

18. Krien, G.; Licht, H. H. and Zierath, J., “Thermochemische Untersuschungen an Nitraminen,” Thermochimica ACTA, Vol. 6. 1973, pp. 465-474.

19. Rylance, J. and Stubley, D., “Heat Capacities and Phase Transactions of Octahydro – 1,3,5,7-Tetranito - 1, 3, 5, 7 – Tetra Zocine,” Thermochimica ACT, Vol. 13, 1975, pp. 253-259.

20. Gustavsen, R. L., Sheffield, S. A., and Alcorn, R. R., “Shock Initiation of ‘Virgin’ and ‘Recycled’ PBX-9502 Measured with Embedded Electro Magnetic Particle Velocity Gauges,” Paper in Proceedings of The Shock Compression of Condensed Matter – 2003 Conference, Edited by M. D. Furnish, Y. M. Gupta, and J. W. Forbes, Published as AIP Conference Proceedings 706, 2004, pages 973-976.

APPENDIX A
COMPUTATION OF M_{AV} AND D_{1AV} FOR PBX-9502

APPENDIX A

Computation of m_{AV} and d_{1av} for PBX-9502

The solid materials considered in this study were chemical mixtures. For these mixtures, the weighted average mass, m_{AV}, of a single atom in the material was desired.

First, it was necessary to compute the mass of a single atom for each of the elements contained in the solid. Each solid was composed of one or more of the following elements:

Carbon, C; Hydrogen, H; Nitrogen, N; Oxygen, O; Chlorine, Cl; Flourine, F.

The mass of a single atom of these elements is:

$$m = \frac{MW}{N_{AV}} = \frac{\text{gram/(gram - mole)}}{\text{atoms/(gram - mole)}} = \frac{\text{grams}}{\text{atom}} \qquad \text{[A-1]}$$

Where:

$$MW = \frac{\text{grams}}{\text{gram - mole}}$$

$$Nav = \text{Avagadros Number} = 6.02252 \times 10^{+23} \ \frac{\text{atoms}}{\text{gram - mole}}$$

Table A-1 lists MW and m for each of the elements in the above list. Values of Nav and MW are from various chemistry text books and handbooks.

To compute the average weight (m_{AV}) of an atom in the material, the chemical formula or proportional chemical composition is required. Of course, the weight (m) of each elemental atom must be known, since m_{AV} is just a weighted average of the elemental atoms in the material. The procedure is valid for mixtures of compounds as well as compounds. See References [1 – 3] for examples.

When m_{AV} is computed, then the average space between the atoms (d_{1AV}) is given by the following relation:

$$d_{1av} = \left(\frac{m_{AV}}{\rho_\circ} \right)^{1/3} = \text{cm} \qquad \text{[A-2]}$$

Computations of m_{AV} and d_{1AV} for PBX-9502 are included in this appendix.

Table A-1. Mass of a Single Atom for Selected Elements

Element	MW Grams / Gram - Mole	N_{AV} Atoms / Gram - Mole	m Grams / Atom
Carbon, C	12.011	$6.02252(10^{23})$	$1.9943(10^{-23})$
Hydrogen, H	1.008	$6.02252(10^{23})$	$0.1674(10^{-23})$
Nitrogen, N	14.008	$6.02252(10^{23})$	$2.3259(10^{-23})$
Oxygen, O	16.00	$6.02252(10^{23})$	$2.6567(10^{-23})$
Chlorine, Cl	35.45	$6.02252(10^{23})$	$5.8874(10^{-23})$
Flourine, F	18.9984	$6.02252(10^{23})$	$3.1546(10^{-23})$

Table A-2. PBX-9502 m_{AV} and $d1_{AV}$

Chemical Composition:	$C_{2.30}\, H_{2.23}\, N_{2.21}\, O_{2.21}\, Cl_{0.038}\, F_{0.13}$	[5]

$C_{2.30}$:	$2.30 \times 1.9943(10^{-23})$	=	$4.58689(10^{-23})$	**GRAMS**
$H_{2.23}$	$2.23 \times 0.1674(10^{-23})$	=	$0.37330(10^{-23})$	↓
$H_{2.21}$	$2.21 \times 2.3259(10^{-23})$	=	$5.14024(10^{-23})$	↓
$O_{2.21}$	$2.21 \times 2.6567(10^{-23})$	=	$5.87131(10^{-23})$	↓
$Cl_{0.038}$	$0.038 \times 5.8874(10^{-23})$	=	$0.22372(10^{-23})$	↓
$F_{0.13}$	$0.13 \times 3.1546(10^{-23})$	=	$0.410048(10^{-23})$	↓
	9.118 ATOMS		**16.60560(10^{-23}) GRAMS**	**GRAMS**

m_{AV}	=	$\frac{16.60560(10^{-23})}{9.118}$	=	$1.82118(10^{-23})$ GRAMS/ATOM

For ρ_O	=	<u>1.891 GRAMS/CC</u>

$d1_{AV}^3$	=	$\frac{m_{AV}}{\rho_\circ}$	=	$\frac{18.2118(10^{-24})}{1.891}$	=	$9.6308(10^{-24})$ CM^3

$d1_{AV}$	=	$2.12759(10^{-8})$ CM	=	2.1276 Å

APPENDIX B
SPECIFIC HEAT (C_P) CONVERSION RELATIONS

Appendix B
Specific Heat (C_P) Conversion Relations

Experimental Specific heat data are usually given in calories (cal) or Joules (J) per molecular weight (MW) per ° centigrade (°C) or ° Kelvin (°K). That is:

$C_P = C_P$ (cal. per MW per ° C or °K)

or

$C_P = C_P$ (J per MW per °C or °K).

Occasionally, C_P is presented as cal. or J per gram °C or °K.

$C_P = C_P$ (cal per gram per °C or °K)

or

Cp = Cp (J per gram per °C or °K)

Note that:

Cp (cal. or J per gram per °C of °K) = Cp (cal, or J per MW per °C or °K)/MW.

Since interest is in Cp (cal or J per atom per °C or °K) then, Cp (cal. or J per atom per °C or °K = m_{AV} Cp (cal. or J per gram per °C or °K).

See Appendix A for procedures to determine m_{AV}. Note that 1° C = 1° K, and that the conversion factor between Joules and calories is 4.184 so that:

Cp (J per atom per °K) = 4.184 * Cp (cal per atom per °K).

Also, since 1 Joule = 10^7 ergs = 10^7 grams (cm/sec) ^{2}

then,

Cp grams ($cm^2/sec^{2)}$ per atom per °K = 10^7. (J per atom per °K).

The above relations were employed in Reference 2, and the present report. However, Cp can also be given in terms of a velocity squared per °K as follows:

Cp(cm^2/sec^2 per °K) = 10^7 x Cp (J per gram per °K). In these units for Cp, $\Delta(\text{v.e.})_{TR} = \int_{T_{EXP}}^{T_R} C_p dT = (\text{cm/sec})^2$, so $U_{PCR1} = \sqrt{\Delta(\text{v.e.})_{TR}}$ = and $U_{PCR2} = \sqrt{2\Delta(\text{v.e})_{TR}} = \sqrt{2}\ U_{PCR1}$.

INITIAL DISTRIBUTION LIST

	Copies
Weapon Systems Technology Information Analysis Center ATTN: Ms. Vakare Valaitis 1901 N. Beauregard Street, Suite 400 Alexandria, VA 22311-1720	1
Defense Technical Information Center 8725 John J. Kingman Rd., Suite 0944 Fort Belvoir, VA 22060-6218	1
Los Alamos National Laboratory ATTN: Dr. Steven A. Sheffield/Dr. R. L. Gustavsen Group DX-1 Mail Stop P-952 Los Alamos, NM 87545	1
Los Alamos National Laboratory ATTN: Dr. Phillip M. Howe Mail Stop 945 Los Alamos, NM 87545	1
Los Alamos National Laboratory ATTN: Roberta Mulford Mail Stop NMT-15 Los Alamos, NM 87545	1
Los Alamos National Laboratory ATTN: Dr. James E. Kennedy Group DX-1 Mail Stop P-950 Los Alamos, NM 87545	1
Los Alamos National Laboratory ATTN: Dr. Douglas G. Tasker Mail Stop J566 Los Alamos, NM 87545	1
Los Alamos National Laboratory ATTN: George Gray III Mail Stop G-755 Los Alamos, NM 87545	1

INITIAL DISTRIBUTION LIST (CONT)

	Copies
Los Alamos National Laboratory ATTN: James N. Johnson/James D. Johnson Mail Stop B-221 Los Alamos, NM 87545	1
Los Alamos National Laboratory ATTN: Blain Asay Mail Stop C-920 Los Alamos, NM 87545	1
Los Alamos National Laboratory ATTN: Joseph N. Fritz DX-1 Mail Stop P-953 Los Alamos, NM 87545	1
Los Alamos National Laboratory ATTN: Dr. Joseph C. Foster, Jr./Dr. Y. Horie 34 Parr Circle Fort Walton Beach, FL 32548	1
Sandia National Laboratory Thermochemical and Physical Division 1534 ATTN: Dr. J. E. Dunn Albuquerque, NM 87185	1
Sandia National Laboratory Computational Physics and Mechanical Division 1531 ATTN: Dr. J. W. Swegle Albuquerque, NM 87185	1
Sandia National Laboratory ATTN: Dr. Mark B. Boslough Shock Wave and Explosion Physics P.O. Box 5800, Division 1153 Albuquerque, NM 87185	1
Sandia National Laboratory P.O. Box 5800, Mail Stop 1033 ATTN: Dr. Douglas Drumheller Albuquerque, NM 87185	1

INITIAL DISTRIBUTION LIST (CONT)

	Copies
Dr. Dennis Hayes Consultant Box 591 Tijeras, NM 87059	1
Sandia National Laboratory Combustion Research Facility Energetic Materials Division ATTN: Dr. Carl F. Melius Livermore, CA 94551	1
Sandia National Laboratory ATTN: Dr. M. D. Furnish/Dr. L. C. Cahabildas Mail Stop 1168 P.O. Box 5800 Albuquerque, NM 87151	1
Sandia National Laboratory ATTN: Marlin E. Kipp Mail Stop 0820 P.O. Box 5800 Albuquerque, NM 87185-0820	1
Mr. Jon Maienschein/Dr. L. Fried/Dr. F. Garcia Lawrence Livermore National Laboratory Mail Code L-282 P.O. Box 808 Livermore, CA 94551	1
Dr. Craig Tarver/Dr. P. A. Urtiew/Dr. K. S. Vandersall Lawrence Livermore National Laboratory Mail Code L-282 P.O. Box 808 Livermore, CA 94551	1
Dr. Neil Holmes Lawrence Livermore National Laboratory Mail Code L-041 P.O. Box 808 Livermore, CA 94551	1

INITIAL DISTRIBUTION LIST (CONT)

	Copies
Dr. William J. Nellis	1
Lawrence Livermore National Laboratory	
Physics Directorate	
700 East Avenue	
Livermore, CA 94550	
U.S. Army ARDEC	
U.S. Army RD&E Command	
ATTN: Mr. Samuel F. Trevino	1
Picatinny Arsenal, NJ 07806-5000	
U.S. Army ATDEC	
Energetic Materials Division, Bldg. 3028	
ATTN: Dr. Surya N. Bulusu	1
Picatinny, NJ 07806-5000	
Naval Surface Warfare Center – Indian Head	
ATTN: Dr. Ruth Doherty	1
101 Strauss Avenue	
Indian Head, MD 20640-5035	
Naval Surface Warfare Center – Dahlgren Division	
ATTN: Dr. Bill Holt/Mr. Daniel Vavrick	1
Code G-22	
17320 Dahlgren Road	
Dahlgren, VA 22448-5100	
Naval Surface Warfare Center – Indian Head	
ATTN: Dr. C. S. Coffey/Dr. J. M. Short	1
101 Strauss Avenue	
Indian Head, MD 20640-5035	
Naval Surface Warfare Center – Carderock	
ATTN: Dr. Jagadish Sharma	1
MacArthur Blvd.	
Bethesda, MD 20817-5700	
Naval Research Laboratory	
Dynamics of Solids Branch	
Condensed Material and Radiation Sciences Division	
ATTN: Mr. Andrew E. Williams	1
Washington, DC 20375	

INITIAL DISTRIBUTION LIST (CONT)

	Copies
Department of the Navy Office of Naval Research ATTN: Dr. Donald Liebenberg 800 North Quincy Street Arlington, VA 22217-5000	1
U.S. Army Research Laboratory ATTN: Dr. Douglas E. Kooker AMSRL-WM-TB Aberdeen Proving Ground, MD 21005-5066	1
U.S. Army Research Laboratory ATTN: Dr. Dattatraya Dandekar Aberdeen Proving Ground, MD 21005-5066	1
Director U.S. Army Research Laboratory SLCRO-MS ATTN: Dr. Kailasam Iyer/Dr. Michael Cistan Research Triangle Park, NC 27709-2211	1
U.S. Army Research Office ATTN: Mr. David Mann P.O. Box 12211 Research Triangle Park, NC 27709-2211	
Eglin Air Force Base ATTN: (AFMC) Dr. Bill Dyess 46 Test Wing Eglin AFB, FL 32542-5910	1
Wright-Patterson Air Force Base ATTN: Dr. Ted Nicholas WRDC-MLLN Wright-Patterson, AFB, OH 45433	1
Director U.S. Army Research Laboratory AMSRD-ARL-WM-TD ATTN: Dr. S. B. Segletes Aberdeen Proving Ground, MD 21995-5066	1

INITIAL DISTRIBUTION LIST (CONT)

	Copies
Director U.S. Army Research Laboratory AMSRD-ARL-SL-BE ATTN: Dr. E. G. Davis Aberdeen Proving Ground, MD 21995-5066	1
California Institute of Technology Division of Geological and Planetary Sciences ATTN: Dr. Thomas J. Ahrens MS-252-21 Pasadena, CA 91125	1
University of Texas at Austin Department of Aerospace Engineering and Engineering Mechanics ATTN: Dr. Byron Tapley W.R. Woolrich Labs Austin, TX 78712-1085	1
University of Dayton Research Institute Impact Physics Group ATTN: Dr. N. S. Brar 300 College Park Avenue Dayton, OH 45469-0182	1
U.S. Naval Academy ATTN: Dr. Mark Ehlert Chemistry Department Annapolis, MD 21402	1
University of California – Los Angeles ATTN: Professor John J. Gilman 6532 Boelter Hall Los Angeles, CA 90024	1
Argonne National Laboratory Technical Information Services Report Unit Bldg. 203 Argonne, IL 60439	1

INITIAL DISTRIBUTION LIST (CONT)

	Copies
Dr. E. R. Fitzgerald Box 291 Monkton, MD 21111	1
Institute for Advanced Technology ATTN: Dr. Stephen Bless/Dr. Harry Fair 4030 Braker Lane, Ste. 200 Austin, TX 78759	1
University of Denver Denver Research Institute ATTN: Mr. Larry Brown Denver, CO 80108	1
Washington State University Institute for Shock Physics Department of Physics ATTN: Dr. Y. M. Gupta/Dr. James R. Asay Pullman, WA 99164-2816	1
Center for Explosive Technology Research Campus Station ATTN: Dr. Pers-Anders Person Socorro, NM 87801	1
Southwest Research Institute Engineering Dynamics Department ATTN: Dr. Charles E. Anderson, Jr./Dr. James Walker P.O. Drawer 28510 San Antonio, TX 78228-0510	1
University of Delaware Department of Chemistry and Biochemistry ATTN: Professor Thomas B. Brill Newark, DE 19716	1
Georgia Institute of Technology School of Materials Science and Engineering ATTN: Dr. N. N. Thadhani 771 Ferst Drive Atlanta, GA 30332-04245	1

INITIAL DISTRIBUTION LIST (CONT)

	Copies
Brown University Division of Engineering ATTN: Dr. R. J. Clifton 182 Hope Street Providence, RI 02912	1
Lynn Barker Valyn International Box 11647 Albuquerque, NM 87192	1
Dr. Leonard I. Stiel Polytechnic University 6 Metrotech Center Brooklyn, NY 11021	1
Dr. Dana D. Dlott University of Illinois 600 S. Matthews Avenue Urbana, IL 61801	1
Alliant, Inc. ATTN: A. Garn Butcher P.O. Box 98 Magna, UT 84037	1
Gencorp Aerojet ATTN: Dr. Joe Carleone P.O. Box 296 1100 West Hollyvale Street Azusa, CA 91702	1
Applied Research Associates, Inc. ATTN: Dr. Dennis D. Grady 4300 San Mateo Blvd., NE. Suite A-220 Albuquerque, NM 87110	1
The Tome Group ATTN: Dr. R. A. Graham 383 Entrada Road Los Lunas, NM 87031	1

INITIAL DISTRIBUTION LIST (CONT)

	Copies
ITT Systems	
ATTN: Dr. James Wilbeck	1
600 Blvd. South, Suite 208	
Huntsville, AL 35815-1506	
Technical Research Corporation	1
P.O. Box 7242	
McLean, VA 22106	
Brigs Company	
ATTN: Joseph E. Backofen	1
2668 Petersborough Street	
Herndon, VA 20171	
Zernow Technical Services, Inc.	
ATTN: Dr. Louis Zernow	1
425 West Bonita Avenue, Suite 208	
San Dimas, CA 91773	
Alan M. Frank and Associates	
ATTN: Dr. Alan M. Frank	1
748 Wimbledon Lane	
Livermore, CA 94559	
SRI International	
ATTN: Dr. Paul DeCarli/Dr. L. Seaman	1
333 Ravenswood Avenue	
Menlo Park, CA 94025	
Dynetics, Inc.	
ATTN: Mr. James Miller	1
1000 Explorer Blvd.	
Huntsville, AL 35806	
Davidson Technologies, Inc.	
ATTN: Mr. Shane Strickland	1
Mr. Brent Deerman	1
Mr. Chris Pitts	1
Ms. Judy Smith	1
530 Discovery Drive	
Huntsville, AL 35806	

INITIAL DISTRIBUTION LIST (CONT)

	Copies
Enig Associates, Inc. ATTN: Mr. Julius W. Enig 12501 Prosperity Drive #340 Silver Spring, MD 20404	1
International Research Associates ATTN: Dr. Dennis L. Orphal 4450 Black Avenue, Suite E Pleasanton, CA 94566	1
Kerley Publishing Services ATTN: Dr. G. I. Kerley P.O. Box 13835 Albuquerque, NM 87192-3835	1
Vitali F. Nestorenko UCSD 9500 Gilman Drive La Jolla, CA 92093-0411	1
Dr. Genau P. Cherepanov 11512 SW 61 Terrace Miami, FL 33373	1
Dr. Julius Roth Consultant 308 Canyon Drive Portola, CA 94025	1
Dr. Franklin E. Walker Interplay 584 W. Treeline Drive Alpine, UT 84994	1
Dr. Muril Robertson Gleason Research Associates 2227 Drake Avenue SW, Suite 2 Huntsville, AL 35805	1

INITIAL DISTRIBUTION LIST (CONT)

		Copies
Dr. Hugh R. James AWE, Aldermaston Bldg. E1 RG7 4PR Reading, Berkshire, UK		1
Dr. Frederic Peugeot Technical Specialist MSIAC, NATO Headquarters B-1110, Brussels Belgium		1
AMSRD-AMR		(Electronic)
AMSRD-AMR-AS-TI,	Mr. Tommy Harris	1
	Mr. Frank Wlodarski	1
AMSRD-AMR-IN-IC		2
AMSRD-AMR-PS-PR,	Dr. W. M. Chew	1
	Mr. Steve Cornelius	1
	Mr. Jay Lilley	1
	Dr. Mike Lyon	1
	Mr. R. W. Milton	1
	Dr. D. M. Thompson	1
AMSRD-AMR-PS-WF,	Mr. Jason Gilliam	1
	Mr. Scott Howard	1
	Mr. Greg Johnson	1
	Dr. Darin Kielsmeier	1
	Mr. Donald Lovelace	1
	Mr. Adolphus McDonald	1
	Mr. Allen Stults	1
	Mr. Paul Turner	1
AMSRD-AMR-SG-RF,	Dr. Brian Smith	1
AMSRD-AMR-SS,	Mr. George Landingham	1
	Mr. Greg Tackett	1
AMSRD-AMR-SS-AT,	Mr. Richard Kretzschmar	1

INITIAL DISTRIBUTION LIST (CONCLD)

		Copies
AMSRD-AMR-SS-AV,	Mr. Steve Low	1
AMSRD-AMR-SS-EG,	Dr. J. P. Billingsley	5
	Mr. Jason Brister	1
	Mr. Dustin Clark	1
	Ms. Edith Crow	1
	Mr. Brian Harrison	1
	Ms. Ann Kissell	1
	Ms. Susan Parker	1
	Mr. Allen Pike	1
	Mr. Glenn Romanczuk	1
	Mr. William Schrenk	1
	Mr. Dan Shady	1
	Ms. Kimberly Williams	1
AMSRD-AMR-SS-HW,	Mr. Alex Jolly	1
AMSRD-AMR-SS-MD,	Mr. James Grabney/Mr. Brad Gass	1
AMSRD-AMR-SS-TM,	Mr. Scott Speigle/Mr. Joseph Webb	1
AMSRD-AMR-WS,	Dr. J. S. Bennett/Dr. Holloman	1
AMSRD-L-G-I,	Mr. Dayn Beam	1
SFAE-MSL-CWS-E,	Mr. Al Dykstra	1
SFAE-MSLS-JAMS,	Mr. Chuck Allen/Mr. Ralph Parker	1